nature neuroscience

CREB regulates excitability and the allocation of memory to subsets of neurons in the amygdala

Yu Zhou[1–4,7], Jaejoon Won[1–4], Mikael Guzman Karlsson[1–4], Miou Zhou[1–4], Thomas Rogerson[1–4], Jayaprakash Balaji[1–4], Rachael Neve[5], Panayiota Poirazi[6] & Alcino J Silva[1–4]

The mechanisms that determine how information is allocated to specific regions and cells in the brain are important for memory capacity, storage and retrieval, but are poorly understood. We manipulated CREB in a subset of lateral amygdala neurons in mice with a modified herpes simplex virus (HSV) and reversibly inactivated transfected neurons with the *Drosophila* allatostatin G protein–coupled receptor (AlstR)/ligand system. We found that inactivation of the neurons transfected with HSV-CREB during training disrupted memory for tone conditioning, whereas inactivation of a similar proportion of transfected control neurons did not. Whole-cell recordings of fluorescently tagged transfected neurons revealed that neurons with higher CREB levels are more excitable than neighboring neurons and showed larger synaptic efficacy changes following conditioning. Our findings demonstrate that CREB modulates the allocation of fear memory to specific cells in lateral amygdala and suggest that neuronal excitability is important in this process.

Memory is thought to depend on specific sets of connected neurons that, together, support the 'memory trace'. Previous results have demonstrated that only a portion of eligible neurons in a network participate in a given memory. For example, approximately 70% of lateral amygdala neurons receive the sensory input involved in tone conditioning, but less than 25% are thought to encode this form of conditioning[1–6]. Why are some neurons, rather than their neighbors, recruited to store a given memory? Recent results suggest that the transcription factor CREB (cyclic adenosine 3′,5′-monophosphate response element binding protein) is crucial for determining which neurons in lateral amygdala take part in encoding an auditory fear memory; neurons with relatively higher CREB levels are preferentially recruited into fear memory traces[5,6]. In this study, we used cell-specific molecular manipulations and inducible and reversible inactivation of targeted cells to study the molecular basis of memory allocation in amygdala neurocircuits. At the heart of our approach is the transfection of a subset of neurons in the amygdala with a viral vector that includes a fluorescently tagged *Creb1* gene and a receptor system that allowed us to reversibly silence those neurons. We found that the virally manipulated CREB biased the allocation of memory to the transfected neurons, as silencing those neurons had a disproportionate effect on memory. Notably, we also found that neurons with higher CREB levels were more excitable than neighboring neurons and experienced larger synaptic efficacy changes following conditioning.

RESULTS

We used a neurotropic, replication-defective HSV[7] to coexpress green fluorescent protein (GFP)-tagged CREB and the *Drosophila* AlstR[8] (HSV-CREB virus; **Fig. 1a**) in a subset of lateral amygdala neurons. The activation of AlstRs has been shown to turn on endogenous mammalian G protein–coupled inwardly rectifying K^+ (GIRK) channels. On binding to its ligand (allatostatin), AlstR/GIRK complexes cause membrane hyperpolarization and, consequently, a decrease in neuronal excitability[8]. As previous studies have found that there is abundant expression of GIRK channels in the amygdala[9], we expected that the activity of HSV-CREB–transfected neurons in tone-conditioned mice could be manipulated by local infusion of allatostatin[10,11]. As a control, we also used a virus that expressed GFP-tagged β-galactosidase (LacZ) instead of GFP-tagged CREB (HSV-LacZ virus; **Fig. 1a**). These viruses were microinjected into lateral amygdala, which is essential for auditory Pavlovian fear conditioning[9,10].

Histological staining with an antibody to GFP revealed that ~20% of lateral amygdala neurons were transfected with virus and that the majority of transfected cells were in the lateral amygdala (**Fig. 1b**). No significant difference was observed between the infection rates for the HSV-CREB and HSV-LacZ viruses (18 ± 3% versus 21 ± 4%, $n = 4$ mice per group, $P > 0.05$). Cannula placement was confirmed with crystal violet staining at the end of each experiment (**Supplementary Fig. 1**). Only those mice with bilateral placements in the basolateral complex of the amygdala were used for analysis. Notably, western blot analyses indicated that HSV-CREB viral transfection increased CREB levels in the amygdala; transfection with HSV-LacZ had no detectable effect on CREB expression (**Supplementary Fig. 2**).

We first determined whether lateral amygdala neurons transfected with either the HSV-CREB or the HSV-LacZ virus could be selectively silenced by allatostatin administration. Whole-cell patch-clamp

[1]Department of Neurobiology, [2]Semel Institute, [3]Department of Psychology, [4]Brain Research Institute, University of California Los Angeles, Los Angeles, California, USA. [5]Picower Institute, Massachusetts Institute of Technology, Cambridge, Massachusetts, USA. [6]Computational Biology Laboratory, Institute of Molecular Biology and Biotechnology (IMBB), Foundation of Research and Technology Hellas, Vassilika Vouton, Heraklion, Crete, Greece. [7]Present address: Department of Physiology, Medical College of Qingdao University, Qingdao, China. Correspondence should be addressed to A.J.S. (silvaa@mednet.ucla.edu).

Received 11 June; accepted 26 August; published online 27 September 2009; doi:10.1038/nn.2405

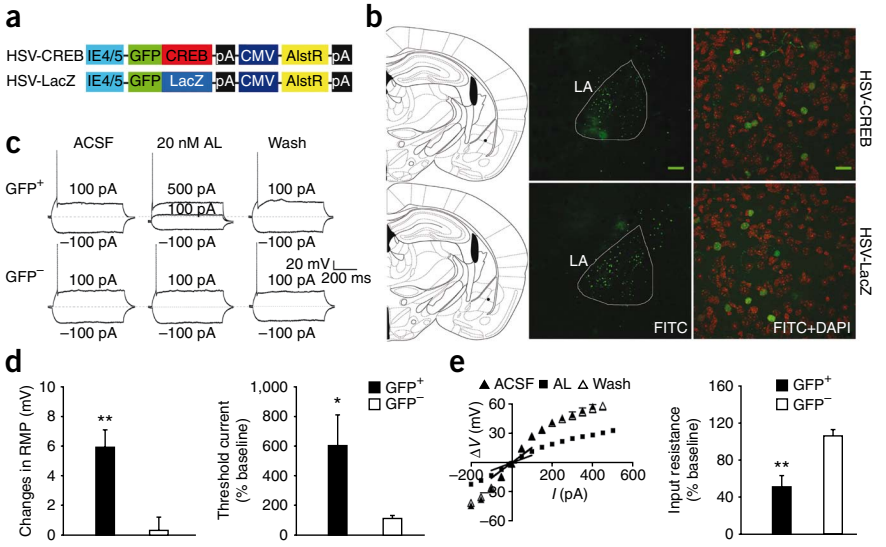

Figure 1 Selective and reversible modulation of a set of genetically targeted lateral amygdala neurons. (**a**) Schematic of the viral amplicons. (**b**) Robust and localized GFP expression in lateral amygdala following HSV-CREB (top) and HSV-LacZ virus infection (bottom). Left, illustration of cannula tip locations (black dot in lateral amygdala) of the representative brain slices (middle). Middle, low-magnification images showing GFP expression (green) in lateral amygdala following virus infection. Scale bar represents 120 μm. Right, high-magnification images showing GFP expression in lateral amygdala neurons. Transfected lateral amygdala cells were stained with both GFP (green) and DAPI (red). Scale bar represents 20 μm. (**c**) Representative traces showing that allatostatin (20 nM) quickly (~5 min) and reversibly inactivated transfected (GFP$^+$) lateral amygdala pyramidal neurons, whereas it had no effect on neighboring nontransfected (GFP$^-$) neurons in the same slices. The dashed line represents the resting potential at –60 mV. The currents injected are shown next to associated traces. ACSF, artificial cerebrospinal fluid. (**d**) Summary of the selective effect of allatostatin on resting membrane potential (RMP, left) and the spike current threshold (right) of transfected lateral amygdala neurons. (**e**) The selective effect of allatostatin (AL) on input resistance of transfected lateral amygdala neurons. Left, *I-V* curves and linear regression used to calibrate input resistance. Right, summary of the selective effects of allatostatin. In **c**–**e**, the transfected neurons include both HSV-CREB and HSV-LacZ neurons. Only about two neurons were recorded from the same slice. $n = 12$–16 cells from four mice for each experimental group. Unpaired *t* test, * $P < 0.05$ and ** $P < 0.01$.

recordings were performed in both visually identified GFP-positive neurons and GFP-negative neighboring cells in the same brain slices from HSV-CREB or HSV-LacZ mice. Consistent with previous studies[12], we found that allatostatin administration quickly and reversibly caused the membrane potential to become more negative (−5.9 ± 1.2 mV, $t = 3.73$, $P < 0.01$) in GFP-positive neurons, but had no effect on the membrane potential of GFP-negative neighboring cells (−0.3 ± 0.9 mV). Moreover, allatostatin administration quickly and reversibly increased the spike current threshold (600 ± 210% of the baseline, $t = 2.33$, $P < 0.05$) and decreased the input resistance (51 ± 12% of the baseline, $t = 3.96$, $P < 0.01$) of GFP-positive lateral amygdala neurons, whereas it had no effect on GFP-negative neurons (**Fig. 1c–e**).

Cell-specific disruption of fear memory in HSV-CREB mice

Next, we determined whether inactivation of the subpopulation of lateral amygdala neurons transfected with HSV-CREB disrupted memory for tone conditioning. If higher levels of CREB expression disproportionally commit transfected neurons to encoding the memory for tone fear conditioning[5,6], then inactivation of these neurons should have a much greater effect on recall than inactivation of neurons transfected with the control HSV-LacZ virus. To test this hypothesis, we bilaterally micro-infused both virus preparations into the lateral amygdala ~3 d before tone fear conditioning[5]. Memory for tone conditioning was assessed by measuring the percentage of time that the mice spent freezing during a tone presentation conducted

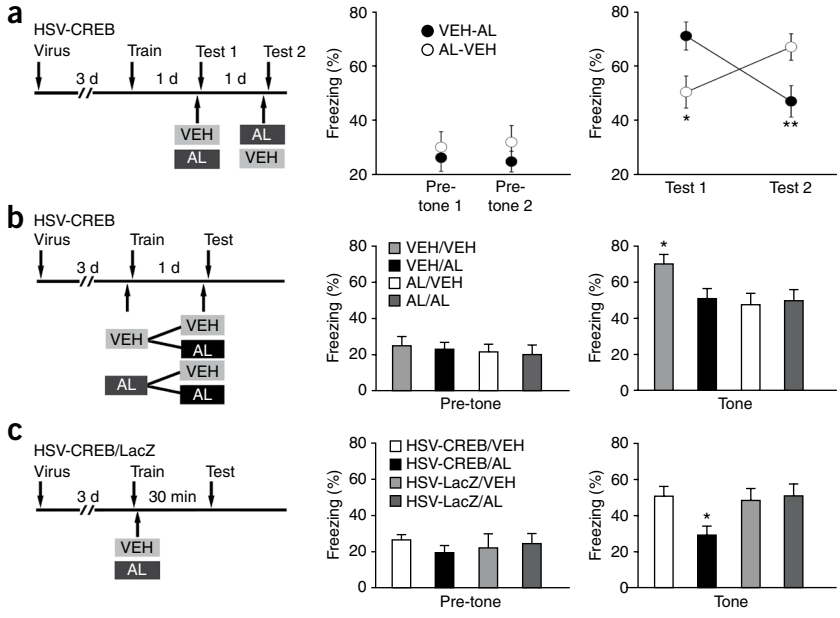

Figure 2 Local infusion of allatostatin selectively impairs auditory fear memory in HSV-CREB mice. Left, schematic of the experimental design. Middle, measurements of freezing before tone presentation (pre-tone). Right, measurements of freezing during tone presentation (tone). (**a**) The effect of allatostatin was reversible. Mice were tested twice (test 1 and test 2), 1 d apart. The vehicle (VEH)-allatostatin (AL) group ($n = 17$) represents mice that received vehicle during test 1 and allatostatin during test 2. The AL-VEH group ($n = 15$) had the opposite treatment. ** $P < 0.01$ and * $P < 0.05$. (**b**) Although allatostatin during testing impaired freezing in mice free of allatostatin during training (VEH/AL versus VEH/VEH), it had no effect in mice that received allatostatin during training (AL/AL versus AL/ VEH). VEH/VEH or AL/AL represent mice that received vehicle or allatostatin during both training and testing. VEH(AL)/AL(VEH) represent VEH(AL) during training and AL(VEH) during testing. $n = 12$ mice for each experimental group. One-way ANOVA, $F_{3,44} = 2.96$, Fisher's PLSD. (**c**) Allatostatin selectively blocked short-term fear memory in HSV-CREB mice. Fisher's PLSD, $n = 12$ mice for each group.

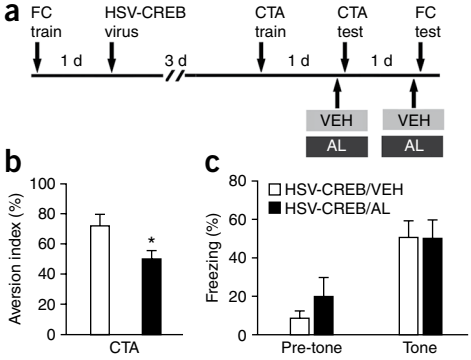

Figure 3 Allatostatin does not disrupt conditioning in HSV-CREB mice established before viral transfection. (**a**) Schematic of the experimental design. Mice were trained on fear conditioning (FC) 1 d before viral transfection and on CTA 3 d after viral transfection. (**b**) Allatostatin infusion impaired CTA memory, which was generated after virus infusion (training after virus infusion). The aversion index is defined as (milliliters of water consumed)/(milliliters of water + milliliters of saccharin consumed) × 100%. The higher the aversion index, the more the mice preferred water to saccharin and the better the CTA memory. Unpaired *t* test, $^*P < 0.05$. (**c**) Allatostatin had no effect on established tone fear conditioning memory (training before virus infusion). Pre-tone, freezing before tone presentation; tone, freezing during tone presentation. $n = 9$ mice for allatostatin group and $n = 6$ mice for vehicle group.

24 h after conditioning. To test the effect of inactivating transfected neurons, we bilaterally infused allatostatin (10 μM, 0.5 μl) or vehicle into the lateral amygdala ~30 min before the retrieval of auditory fear memory. Notably, mice transfected with HSV-CREB (HSV-CREB mice) and treated with allatostatin showed less freezing (41.4 ± 3.7%, $t = 2.58$, $P < 0.05$) than HSV-CREB mice treated with saline (65.3 ± 8.5%), whereas allatostatin had no effect on freezing of the HSV-LacZ mice (**Supplementary Fig. 3**).

As a control, we also infused allatostatin or vehicle into the lateral amygdala of separate groups of mice and waited 4 h (instead of 30 min) before testing tone conditioning (**Supplementary Fig. 4**). We found that allatostatin infusion 4 h before testing had no effect on retrieval, indicating that the effect of allatostatin *in vivo* lasts at least 30 min, but no longer than 4 h. In addition, the absence of a memory effect in mice that received the control virus strongly suggests that allatostatin did not have a nonspecific effect on lateral amygdala neuronal function. Thus, these data support the hypothesis that neurons with higher CREB expression are disproportionally engaged in the neuronal representation that encodes tone fear memory in the lateral amygdala.

To test whether the effects of allatostatin are reversible, we repeated the experiment just described, but added a second test 24 h after the first test. In the second test, we reversed the treatments so that the mice that were infused with allatostatin in the first test were infused with vehicle in the second test (and vice versa). We found (**Fig. 2a**) that the effects of allatostatin were fully reversible, as HSV-CREB mice treated with allatostatin in the first test (test 1, 50.7 ± 5.7% freezing) showed normal freezing in the second test (test 2, 67.1 ± 5.1%, $t = 2.14$, $n = 15$, $P < 0.05$) when treated with saline. In addition, HSV-CREB mice treated with saline in the first test (71.1 ± 4.8% freezing) showed a memory impairment (freezing time: 47.3 ± 5.8%, $t = 3.17$, $n = 17$, $P < 0.01$ compared with test 1) when treated with allatostatin in the second test.

If higher CREB expression increases the probability that neurons in the lateral amygdala encode the tone memory[5], then inactivating those neurons during tone conditioning should prevent them from participating in the encoding process, and consequently preclude HSV-CREB from biasing memory allocation. To test this hypothesis, we included an allatostatin manipulation during both training and testing (**Fig. 2b**). Consistent with CREB's role in memory consolidation[13,14], we found that activation of the HSV-CREB neurons during training enhanced tone-associated fear memory (vehicle/vehicle, 70.0 ± 5.5%, $n = 12$), whereas inactivation of the HSV-CREB neurons with allatostatin during training reduced tone-associated fear memory to control levels (allatostatin/vehicle, 47.4 ± 6.4%, $n = 12$; **Fig. 2b**). Notably, we found that, although allatostatin during testing disrupted freezing in mice that received saline during training (vehicle/allatostatin versus vehicle/vehicle), the same treatment

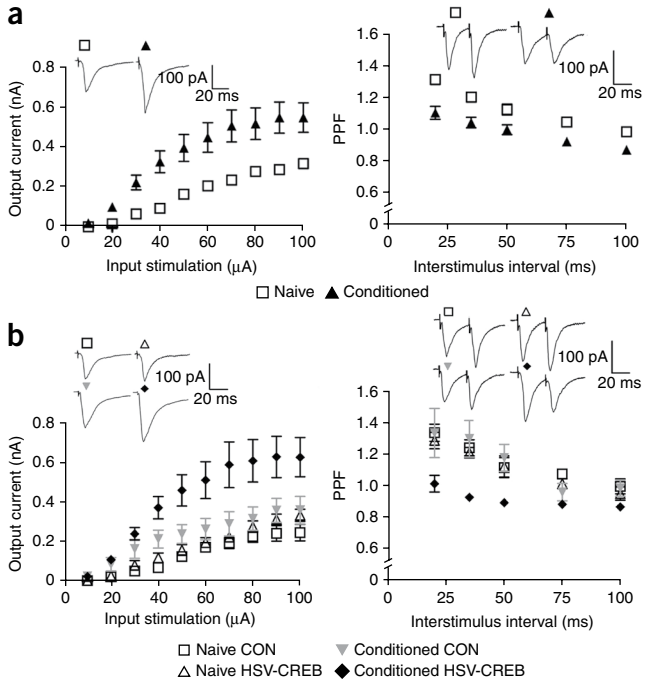

Figure 4 HSV-CREB neurons in conditioned mice show increased synaptic efficacy. (**a**) Comparison of lateral amygdala synaptic properties in naïve (untrained) versus conditioned (trained) mice. Left, evoked EPSCs in thalamo-lateral amygdala synapses were enhanced after conditioning. Two-way ANOVA, $F_{1,37} = 7.68$, $P < 0.01$ (naive, $n = 15$ neurons; conditioned, $n = 24$ neurons from 6 mice per group). Right, PPF was decreased in thalamo-lateral amygdala synapses after conditioning. Two-way ANOVA, $F_{1,82} = 26.35$, $P < 0.001$ (naive, $n = 37$ neurons; conditioned, $n = 47$ neurons from 8 mice per group). (**b**) Comparison of lateral amygdala synaptic properties in naive versus conditioned mice transfected with HSV-CREB virus. Naive CON and conditioned CON refer to nontransfected (GFP negative) lateral amygdala neurons, whereas naive HSV-CREB and conditioned HSV-CREB refer to transfected (GFP positive) neurons from naive and conditioned mice. Left, HSV-CREB neurons ($n = 12$) showed increased synaptic EPSCs after conditioning compared with other groups (naive CON, $n = 5$; naive HSV-CREB, $n = 7$; conditioned CON, $n = 8$, from 5–6 mice per group). One-way repeated ANOVA, $P < 0.001$; Newman-Keuls multiple comparison test, $P < 0.001$. Right, HSV-CREB neurons showed decreased PPF after conditioning. HSV-CREB neurons, $n = 13$; naive CON, $n = 10$; naive HSV-CREB, $n = 11$; conditioned CON, $n = 8$, from 6 mice per group. One-way ANOVA, $P < 0.001$; Newman-Keuls multiple comparison test, $P < 0.001$. Inserts, sample traces from different neurons as indicated. The stimulation intensity was 30 μA and the interstimulus interval in PPF was 35 ms.

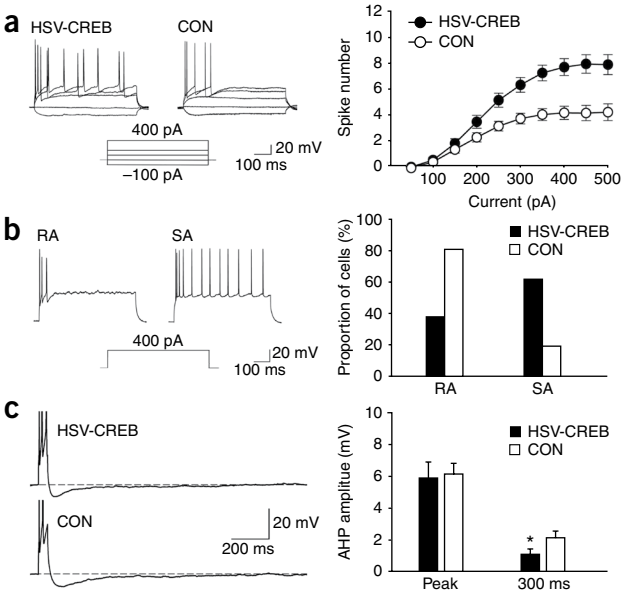

Figure 5 CREB increases neuronal excitability in transfected lateral amygdala neurons. (**a**) Left, traces of sample recordings showing more action potentials in response to increasing current injections (−100, 0, 100, 200 and 400 pA; 600 ms) in a HSV-CREB neuron than in a neighboring nontransfected neurons (CON). Right, we found significantly more action potentials in HSV-CREB neurons ($n = 58$, from 8 mice) than in controls ($n = 64$, from 12 mice from the other three groups, repeated ANOVA, $P < 0.05$). (**b**) HSV-CREB changed the firing properties of transfected lateral amygdala pyramidal neurons. Left, sample voltage traces showing two lateral amygdala neurons with distinct firing properties[24]. Rapidly adapting (RA) cells fired only 1–5 spikes at the onset of the current injection (600 ms, 400 pA) and remained silent for the rest of the current pulses. Slowly adapting (SA) cells fired more than six spikes. Right, distribution of firing properties of HSV-CREB neurons and control lateral amygdala neurons. (**c**) HSV-CREB neurons showed reduced post-burst AHP compared with control neurons. Left, sample post-burst AHP traces from a HSV-CREB neuron and a neighboring control neuron. Right, histogram showing AHP difference between HSV-CREB neurons ($n = 58$, from 8 mice) and the control neurons ($n = 64$, from 12 mice from the other three groups) as measured at peak and 300 ms after the end of current step. Unpaired t test, * $P < 0.05$.

did not affect freezing in mice that received allatostatin during training (allatostatin/allatostatin, 49.5 ± 6.6%; allatostatin/vehicle, 47.4 ± 6.4%; $n = 12$ per group, Fisher's PLSD, $P > 0.05$; **Fig. 2b**). This result indicates that allatostatin administration during testing does not affect memory retrieval in mice treated with allatostatin during training, demonstrating that HSV-CREB can only affect memory allocation when transfected cells are active during training. Altogether, these results indicate that neuronal activation during training is crucial for CREB's role in memory allocation.

Because our measures of memory allocation were taken at least 24 h after training (**Fig. 2a**,**b**), it is possible that the well-known effects of CREB on memory consolidation[13,14] could be confounding our interpretation of CREB's role on memory allocation. Thus, we tested memory allocation 30 min after training, a time point that is known to precede memory consolidation[13,14]. Indeed, when tested 30 min post-training, HSV-CREB mice did not show higher freezing than HSV-LacZ mice, indicating that HSV-CREB does not enhance tone fear memory 30 min post-training (**Fig. 2c**). Nevertheless, local administration of allatostatin immediately after training did disrupt 30-min memory for tone conditioning in HSV-CREB mice (HSV-CREB/vehicle, 50.9 ± 5.5%; HSV-CREB/allatostatin, 28.9 ± 5.2%; $F_{3,44} = 6.93$, Fisher's PLSD, $P < 0.05$, $n = 12$ per group), whereas it had no effect on HSV-LacZ mice (HSV-LacZ/vehicle, 48.1 ± 7.5%; HSV-LacZ/allatostatin, 52.9 ± 5.7%; **Fig. 2c**). These findings indicate that CREB's role in memory allocation cannot be attributed to its effects on memory consolidation. In addition, memory allocation was observed as early as 30 min following training. Previous results have suggested that transfection with HSV-CREB does not recruit more lateral amygdala neurons during encoding and that the total number of lateral amygdala neurons involved in a specific memory remains unchanged across various CREB manipulations[5,6]. This implies that our tone fear results 24 h after training are not simply the result of silencing of neurons driven into the amygdala memory trace by HSV-CREB.

To test the behavioral specificity of the HSV-CREB effects on memory, we repeated the experiments described above with two important modifications. First, we fear-conditioned the mice before (and not after) viral injection. Second, we trained the same mice on taste aversion conditioning (CTA) 3 d after viral infection (**Fig. 3**). We chose CTA because it also depends on the amygdala[15–17]. As predicted, we found that allatostatin infusion impaired CTA memory (HSV-CREB/vehicle, 71.9 ± 7.7%; HSV-CREB/allatostatin, 50.0 ± 5.9%; $t = 2.31$, $P < 0.05$; **Fig. 3b**), but had no effect on tone fear memory (HSV-CREB/vehicle, 50.6 ± 8.6%; HSV-CREB/allatostatin, 49.9 ± 9.8%, $P > 0.05$; **Fig. 3c**). Notably, the total levels of fluid consumption in CTA test were the same in different treatment groups. These data demonstrate the behavioral specificity of the HSV-CREB effects and indicate that pre-training, but not post-training, HSV-CREB infusions affects memory allocation in lateral amygdala. These data also demonstrate that CREB has a role in the allocation of memory for CTA, suggesting that our findings may be generally applicable to amygdala-dependent learning.

HSV-CREB neurons show increased synaptic efficacy

Previous studies in thalamo-lateral amygdala synapses following tone fear conditioning found that synaptic transmission was increased and paired-pulse facilitation (PPF) was decreased[18,19]. To test whether HSV-CREB neurons in lateral amygdala are preferentially recruited to encode fear memory, we studied synaptic transmission and PPF in HSV-CREB neurons and nontransfected neighboring cells in the same brain slices in both naive and conditioned mice (24 h post-training). Consistent with previous findings[18,19], our whole-cell recording

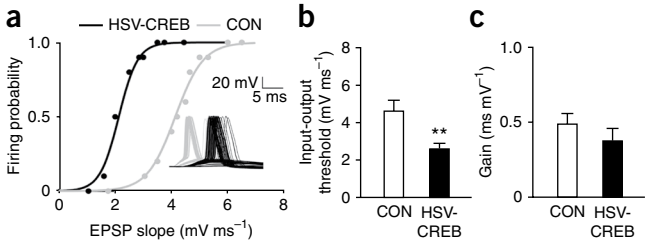

Figure 6 HSV-CREB changes the input-output function of transfected lateral amygdala neurons. (**a**) Unit E-S curve of a HSV-CREB neuron and a neighboring nontransfected neuron (CON). Insert, representative EPSPs and action potentials traces from a HSV-CREB and a CON neuron following increasing synaptic stimulations. (**b**) HSV-CREB lowered the input-output threshold in transfected lateral amygdala neurons. The threshold was quantified as the EPSP slope (mV ms^{-1}) corresponding to 50% firing probability. (**c**) HSV-CREB did not change the slope (gain) of the linear component of the E-S curve. HSV-CREB, $n = 10$; CON, $n = 11$ from 5 mice. Unpaired t test, * $P < 0.01$.

studies in the thalamo-lateral amygdala pathway showed that fear conditioning potentiated synaptic transmission (two-way ANOVA, $F_{1,37} = 7.68$, $P < 0.01$; **Fig. 4a**) and decreased PPF (two-way ANOVA, $F_{1,82} = 26.35$, $P < 0.001$; **Fig. 4a**).

We found that HSV-CREB neurons in conditioned mice (conditioned HSV-CREB) had both enhanced synaptic transmission and reduced PPF when compared with the other three control groups, which included neighboring neurons without viral transfection in conditioned mice (conditioned CON), HSV-CREB neurons (naive HSV-CREB) and neighboring nontransfected neurons (naive CON) in naive mice (one-way repeated-measures ANOVA, $P < 0.001$; **Fig. 4b**). Statistical analysis showed that the evoked excitatory postsynaptic currents (EPSCs) and PPF in conditioned HSV-CREB neurons were significantly different from the other three groups (Newman-Keuls multiple comparison test, $P < 0.001$). On the contrary, although the evoked EPSCs in conditioned CON neurons were also different from those of naive HSV-CREB and naive CON neurons ($P < 0.05$–0.01), the average PPFs among those three groups were identical ($P > 0.05$). Both synaptic EPSCs and PPF were indistinguishable in the naive HSV-CREB and naive CON groups, indicating that HSV-CREB did not change evoked basal synaptic transmission and PPF at thalamo-lateral amygdala synapses in naive, unconditioned mice. Taken together, these data provide additional evidence for the hypothesis that neurons with higher CREB function are disproportionally engaged in neuronal representations that encode tone fear memory in the lateral amygdala.

HSV-CREB neurons show increased neuronal excitability

How could neurons with higher CREB levels bias memory allocation? It is possible that higher levels of CREB expression lead to increased expression of specific channels and signaling proteins that increase the excitability of these neurons[20–22], thereby increasing the probability that they are recruited during learning. To test this hypothesis, we prepared acute lateral amygdala slices ~3 d after virus infusion and performed whole-cell recordings. We found that, although HSV-CREB did not affect the resting membrane potential, input resistance, spike amplitude or the spike half-width of transfected lateral amygdala pyramidal neurons (**Supplementary Table 1**), it did significantly lower the action potential threshold of those neurons (HSV-CREB, −38.8 ± 0.9 mV; one-way ANOVA, $P < 0.05$ compared with the other three control groups, −35.4 ± 1.0 mV to −35.7 ± 1.0 mV; **Supplementary Table 1**). In addition, HSV-CREB caused a robust increase in the number of action potentials elicited by depolarizing current injections; in HSV-CREB neurons ($n = 58$, from eight mice), the number of action potentials triggered by depolarizing current injections was higher than in nontransfected neurons or in neurons transfected with the HSV-LacZ control virus (repeat ANOVA analysis, $P < 0.05$; **Fig. 5a**). Accordingly, HSV-CREB neurons showed a reduced spike-frequency adaptation; analysis of the distribution of neuronal firing properties indicated that 62% (36 out of 58) of HSV-CREB neurons fired more than six spikes in response to a 400-pA, 600-ms current injection, whereas only 19% (12 out of 64) of control neurons did so (**Fig. 5b**). Altogether, the decreased spike threshold, increased number of action potentials and reduced spike frequency adaptation indicate that HSV-CREB neurons have increased intrinsic excitability. Because the afterhyperpolarization (AHP) is also known to affect excitability[23–27], we measured the post-burst AHP of HSV-CREB and control neurons at two time points: the negative peak and 300 ms after the end of the current pulse. We found that HSV-CREB neurons had a significant (one-way ANOVA, $P < 0.05$) reduction in the amplitude of the AHP at 300 ms after the current pulse, but not at peak amplitude (**Fig. 5c**), suggesting that later components of the AHP may be specifically affected by HSV-CREB.

Next, we determined whether the intrinsic excitability changes in HSV-CREB neurons alter the input-output function of neurons, an important property for information processing during learning. We measured the relationship between the excitatory postsynaptic potential (EPSP) slope and spike probability following different synaptic stimulation intensities (the E-S curve) in HSV-CREB–transfected and neighboring control neurons. We observed a leftward shift of the E-S curve in HSV-CREB neurons (HSV-CREB, 2.6 ± 0.3 mV ms^{-1}; CON, 4.6 ± 0.6 mV ms^{-1}; $P < 0.01$; **Fig. 6**). Specifically, we found a decrease in the EPSP slope that yields action potentials with 50% probability, which can be explained by a lower threshold for action potential generation in HSV-CREB cells (**Supplementary Table 1**). In contrast, the slope of the E-S curve was not changed. This result indicates that HSV-CREB neurons have stronger EPSP spike coupling.

Previous studies showed that both changes in synaptic strength (LTP) and changes in intrinsic excitability could lead to a left shift of the E-S curve[28–30]. Our whole-cell recordings in HSV-CREB and neighboring nontransfected neurons showed that HSV-CREB did not change evoked basal synaptic transmission and PPF at thalamo-lateral amygdala synapses in naive mice (**Fig. 4b**). In addition, there was no detectable difference in the AMPA/NMDA EPSC ratio between HSV-CREB and HSV-LacZ neurons (**Supplementary Fig. 5**). Consistently, HSV-CREB expression did not change the slope of the E-S curve (**Fig. 6**), suggesting that inhibition was not changed[28–30]. Thus, the E-S potentiation that we observed in HSV-CREB neurons is probably a result of changes in the intrinsic electrical properties of postsynaptic neurons. Our analyses of intrinsic and synaptically driven excitability in naive mice indicate that HSV-CREB increases the excitability of lateral amygdala neurons and strengthen their input-output function. These findings provide a possible explanation for the selective role of CREB in memory allocation: neurons with higher CREB levels have higher excitability and are therefore more likely to be recruited in a memory trace.

DISCUSSION

We found that CREB was able to modulate the allocation of fear memory to specific neurons in the lateral amygdala and that neuronal excitability may be important in this process. Because we found that neurons with virally encoded CREB (that is, higher CREB levels) were more excitable, they were more likely to be both activated during conditioning and recruited into storing the conditioning episode. Synchronous or correlated activity with thalamic inputs could in turn lead to the strengthening of thalamo-amygdala connections with these neurons. Indeed, our findings indicate that these synapses are stronger in HSV-CREB neurons from trained mice. Thus, only a specific subset of neurons, the ones with higher levels of CREB expression, and thus higher excitability, will be engaged in the memory trace.

In addition to its involvement in excitability, a large body of evidence suggests that CREB-dependent transcription is essential for both long-lasting forms of synaptic plasticity and long-term memory, but not short-term plasticity or short-term memory[31–35]. Thus, the excitability and synaptic plasticity mediated by CREB will eventually work together to support the memory representation in a subset of neurons of the lateral amygdala.

It is possible that differences in the endogenous levels of CREB activity normally contribute to the diversity of firing properties in projection neurons in the lateral amygdala[24]. Although the *Creb* target genes that are responsible for the changes in excitability that we observed in lateral amygdala neurons are still not known, it is possible that, as has previously been seen in other brain areas[20–22,36], increased CREB expression or activity in the amygdala changes the expression of voltage-dependent ion channels and the second messenger systems

that modulate those channels, and consequently increases the excitability of specific amygdala neurons[37]. This subset of neurons with higher excitability could then be more easily activated during learning and would therefore be more likely to be recruited into specific memory representations. Thus, dynamic regulation of intracellular CREB activity in individual neurons of a network might be one of the crucial organizing principles for memory allocation. Therefore, some or all of the cooperating and antagonizing signaling pathways known to regulate CREB activity might fine tune the process that allocates memories in neuro-networks[37].

Following robust activation of CREB, it is also possible that CREB repressors, such as inducible cAMP early repressor[38], are transcribed. The progressive accumulation of CREB repressors could then have an overall negative effect on CREB activity and therefore on memory allocation. The balance of factors that either promote or dampen neuronal excitability would then control whether two memories are stored in the same or different cells. It is possible that CREB is only one of many factors involved in memory allocation and that excitability is just one of several mechanisms that determine which cells in a network encode a given memory.

Our results provide direct evidence that memory is not evenly stored in neuronal networks[1,2,5,6] and that CREB is involved in determining which subset of neurons is recruited during training. Notably, CREB does not seem to change the total number of neurons in the memory trace[5,6], suggesting that there may be a competitive process that determines cellular participation in the memory trace. At a circuit level, it is possible that there is a relationship between the total number of activated neurons and network inhibition; the initial recruitment of a larger number of neurons would result in stronger inhibition and therefore in a feedback circuit process that limits the total number of cells committed to any one given memory. Our results, along with others[5,6], represent an important step toward unraveling the organizing principles and mechanisms behind the emergence of Hebbian cell assemblies responsible for information storage and retrieval in brain structures such as the amygdala.

METHODS

Methods and any associated references are available in the online version of the paper at http://www.nature.com/natureneuroscience/.

Note: Supplementary information is available on the Nature Neuroscience website.

ACKNOWLEDGMENTS

We thank T. Carvalho, Y.-S. Lee, P. Golshani, D. Buonomano, B. Wiltgen, W. Tan, J. Shobe, J. Feldman and J. Guzowski for helpful advice, E. Callaway for AlstR cDNA and K. Cai for technical support. This work was supported by grants from the US National Institutes of Health (P50-MH0779720 and R37-AG13622) to A.J.S. and a Marie Curie Outgoing fellowship of the European Commission (PIOF-GA-2008-219622) to P.P.

AUTHOR CONTRIBUTIONS

Y.Z., J.W. and A.J.S. designed the experiments. Y.Z., J.W., M.G.K. and T.R. carried out the behavioral experiments. Y.Z. performed the patch-clamp and whole-cell recording experiments. J.W. generated the viral vectors and R.N. provided the viral preparations. M.Z. carried out the western blot analysis. Y.Z. and J.W. analyzed the data. B.J. and P.P. helped with the discussion. Y.Z and A.J.S. wrote the paper.

Published online at http://www.nature.com/natureneuroscience/.
Reprints and permissions information is available online at http://www.nature.com/reprintsandpermissions/.

1. Repa, J.C. *et al.* Two different lateral amygdala cell populations contribute to the initiation and storage of memory. *Nat. Neurosci.* **4**, 724–731 (2001).
2. Rumpel, S., LeDoux, J., Zador, A. & Malinow, R. Postsynaptic receptor trafficking underlying a form of associative learning. *Science* **308**, 83–88 (2005).
3. Reijmers, L.G., Perkins, B.L., Matsuo, N. & Mayford, M. Localization of a stable neural correlate of associative memory. *Science* **317**, 1230–1233 (2007).
4. Schafe, G.E., Doyere, V. & LeDoux, J.E. Tracking the fear engram: the lateral amygdala is an essential locus of fear memory storage. *J. Neurosci.* **25**, 10010–10014 (2005).
5. Han, J.H. *et al.* Neuronal competition and selection during memory formation. *Science* **316**, 457–460 (2007).
6. Han, J.H. *et al.* Selective erasure of a fear memory. *Science* **323**, 1492–1496 (2009).
7. Clark, M.S. *et al.* Overexpression of 5-HT1B receptor in dorsal raphe nucleus using herpes simplex virus gene transfer increases anxiety behavior after inescapable stress. *J. Neurosci.* **22**, 4550–4562 (2002).
8. Birgül, N., Weise, C., Kreienkamp, H.J. & Richter, D. Reverse physiology in *Drosophila*: identification of a novel allatostatin-like neuropeptide and its cognate receptor structurally related to the mammalian somatostatin/galanin/opioid receptor family. *EMBO J.* **18**, 5892–5900 (1999).
9. Karschin, C., Dissmann, E., Stuhmer, W. & Karschin, A. IRK(1–3) and GIRK(1–4) inwardly rectifying K^+ channel mRNAs are differentially expressed in the adult rat brain. *J. Neurosci.* **16**, 3559–3570 (1996).
10. Tan, E.M. *et al.* Selective and quickly reversible inactivation of mammalian neurons *in vivo* using the *Drosophila* allatostatin receptor. *Neuron* **51**, 157–170 (2006).
11. Tan, W. *et al.* Silencing preBotzinger complex somatostatin-expressing neurons induces persistent apnea in awake rat. *Nat. Neurosci.* **11**, 538–540 (2008).
12. Lechner, H.A., Lein, E.S. & Callaway, E.M. A genetic method for selective and quickly reversible silencing of mammalian neurons. *J. Neurosci.* **22**, 5287–5290 (2002).
13. Kida, S. *et al.* CREB required for the stability of new and reactivated fear memories. *Nat. Neurosci.* **5**, 348–355 (2002).
14. Bourtchuladze, R. *et al.* Deficient long-term memory in mice with a targeted mutation of the cAMP-responsive element binding protein. *Cell* **79**, 59–68 (1994).
15. Yamamoto, T., Shimura, T., Sako, N., Yasoshima, Y. & Sakai, N. Neural substrates for conditioned taste aversion in the rat. *Behav. Brain Res.* **65**, 123–137 (1994).
16. Lamprecht, R., Hazvi, S. & Dudai, Y. cAMP response element binding protein in the amygdala is required for long- but not short-term conditioned taste aversion memory. *J. Neurosci.* **17**, 8443–8450 (1997).
17. Josselyn, S.A., Kida, S. & Silva, A.J. Inducible repression of CREB function disrupts amygdala-dependent memory. *Neurobiol. Learn. Mem.* **82**, 159–163 (2004).
18. McKernan, M.G. & Shinnick-Gallagher, P. Fear conditioning induces a lasting potentiation of synaptic currents *in vitro*. *Nature* **390**, 607–611 (1997).
19. Huang, Y.Y. & Kandel, E.R. Postsynaptic induction and PKA-dependent expression of LTP in the lateral amygdala. *Neuron* **21**, 169–178 (1998).
20. Han, M.H. *et al.* Role of cAMP response element-binding protein in the rat locus ceruleus: regulation of neuronal activity and opiate withdrawal behaviors. *J. Neurosci.* **26**, 4624–4629 (2006).
21. Dong, Y. *et al.* CREB modulates excitability of nucleus accumbens neurons. *Nat. Neurosci.* **9**, 475–477 (2006).
22. Viosca, J., Lopez de Armentia, M., Jancic, D. & Barco, A. Enhanced CREB-dependent gene expression increases the excitability of neurons in the basal amygdala and primes the consolidation of contextual and cued fear memory. *Learn. Mem.* **16**, 193–197 (2009).
23. Murphy, G.G. *et al.* Increased neuronal excitability, synaptic plasticity, and learning in aged Kvbeta1.1 knockout mice. *Curr. Biol.* **14**, 1907–1915 (2004).
24. Faber, E.S., Callister, R.J. & Sah, P. Morphological and electrophysiological properties of principal neurons in the rat lateral amygdala *in vitro*. *J. Neurophysiol.* **85**, 714–723 (2001).
25. Storm, J.F. Potassium currents in hippocampal pyramidal cells. *Prog. Brain Res.* **83**, 161–187 (1990).
26. Oh, M.M., McKay, B.M., Power, J.M. & Disterhoft, J.F. Learning-related postburst afterhyperpolarization reduction in CA1 pyramidal neurons is mediated by protein kinase A. *Proc. Natl. Acad. Sci. USA* **106**, 1620–1625 (2009).
27. Santini, E., Quirk, G.J. & Porter, J.T. Fear conditioning and extinction differentially modify the intrinsic excitability of infralimbic neurons. *J. Neurosci.* **28**, 4028–4036 (2008).
28. Staff, N.P. & Spruston, N. Intracellular correlate of EPSP-spike potentiation in CA1 pyramidal neurons is controlled by GABAergic modulation. *Hippocampus* **13**, 801–805 (2003).
29. Carvalho, T.P. & Buonomano, D.V. Differential effects of excitatory and inhibitory plasticity on synaptically driven neuronal input-output functions. *Neuron* **61**, 774–785 (2009).
30. Losonczy, A., Makara, J.K. & Magee, J.C. Compartmentalized dendritic plasticity and input feature storage in neurons. *Nature* **452**, 436–441 (2008).
31. Silva, A.J., Kogan, J.H., Frankland, P.W. & Kida, S. CREB and memory. *Annu. Rev. Neurosci.* **21**, 127–148 (1998).
32. Shaywitz, A.J. & Greenberg, M.E. CREB: a stimulus-induced transcription factor activated by a diverse array of extracellular signals. *Annu. Rev. Biochem.* **68**, 821–861 (1999).
33. Mayr, B. & Montminy, M. Transcriptional regulation by the phosphorylation-dependent factor CREB. *Nat. Rev. Mol. Cell Biol.* **2**, 599–609 (2001).
34. Lonze, B.E. & Ginty, D.D. Function and regulation of CREB family transcription factors in the nervous system. *Neuron* **35**, 605–623 (2002).
35. Carlezon, W.A. Jr., Duman, R.S. & Nestler, E.J. The many faces of CREB. *Trends Neurosci.* **28**, 436–445 (2005).
36. Jancic, D., Lopez de Armentia, M., Valor, L.M., Olivares, R. & Barco, A. Inhibition of cAMP response element binding protein reduces neuronal excitability and plasticity, and triggers neurodegeneration. *Cereb. Cortex* published online, doi:10.1093/cercor/bhp004 (12 February 2009).
37. Won, J. & Silva, A.J. Molecular and cellular mechanisms of memory allocation in neuronetworks. *Neurobiol. Learn. Mem.* **89**, 285–292 (2008).
38. Sassone-Corsi, P. Transcription factors responsive to cAMP. *Annu. Rev. Cell Dev. Biol.* **11**, 355–377 (1995).

ONLINE METHODS

Mice. Adult F_1 hybrid (C57Bl/6NTac × 129S6/SvEvTac) mice were group housed (3–4 per cage) on a 12-h light/dark cycle. Food and water were available *ad libitum* throughout the experiment. All procedures were approved by the Chancellor's Animal Research Committee at the University of California at Los Angeles, in accordance with US National Institutes of Health guidelines.

HSV vectors. Two vectors were used, HSV-CREB-AlstR (HSV-CREB vector) and HSV-LacZ-AlstR (Control vector). Genes of interest (*Creb*, *LacZ* and *AlstR*) were cloned into a bicistronic HSV amplicon[7]. To visualize transgene expression, we fused eGFP to the 5′ end of the CREB and LacZ cDNA. *Creb1* or *LacZ* were expressed from an IE4/5 promoter and *AlstR* from a CMV promoter. The amplicon was packaged according to published methods[39].

Surgery and virus infusion. Mice were pretreated with atropine sulfate (0.1 mg per kg of body weight, intraperitoneal), anesthetized with chloral hydrate (400 mg per kg, intraperitoneal) and placed in a stereotaxic frame. The skin was retracted and holes were drilled in the skull bilaterally above the lateral amygdala (anterior-posterior = −1.3, medial-lateral = ±3.3, ventral = −4.8 mm from bregma) according to a mouse brain atlas[40]. For behavioral experiments, a stainless steel outer cannula (Plastic One) was implanted to lateral amygdala and fixed on the skull with dental cement. After cannula implantation, mice were single-housed and handled every day. Virus infusion was delayed until 7 d after surgery to ensure physical recovery. A virus solution (1.3 µl, bilateral) was delivered to lateral amygdala at a flow rate of 0.065 µl min^{-1} through inner injection cannula (Plastic one, 22 gauge) attached by polyethylene tubing to Hamilton microsyringes mounted in an infusion pump (Harvard Instruments). The infusion cannula was left in place an additional 10 min to ensure diffusion of the vector. For electrophysiological studies, virus solution (1.3 µl) was delivered to lateral amygdala over 5 min through glass micropipettes (Sutter Instrument) immediately after the holes were drilled. The micropipette was left in place for 5 min post-injection. Electrophysiological or behavioral experiments were performed 3 d following virus infusion[41].

Allatostatin administration. The peptide allatostatin[12] (New England) was dissolved in ddH_2O to make a 2.5 mM stock solution. Saline was added to dilute it to the proper final concentration for each specific experiment. Allatostatin solution (0.5 µl), or the same amount of vehicle (saline), was delivered bilaterally to the lateral amygdala of awake mice at a flow rate of 0.25 µl min^{-1} through inner injection cannula. The cannula was left in place for 2 min post-injection. Behavioral procedures were started ~30 min after injection.

Auditory (tone) fear conditioning. Training consisted of placing the mice in a conditioning chamber (context A) and presenting a tone 2 min later (2,800 Hz, 85 dB, 30 s) that terminated with a shock (2 s, 0.5 mA). Mice remained in the chamber for an additional minute. The mice were tested for auditory fear conditioning either 30 min or 24 h later. Mice were placed in a novel chamber (context B) and the tone conditioned stimulus was presented (for 1 min) 2 min later. Our index of memory, freezing (the cessation of all movement except for respiration), was assessed via an automated scoring system (Med Associates) with a 30 frames per s sampling; the mice needed to freeze continuously for at least 1 s before freezing could be counted. The same training protocol was also used in the electrophysiological studies. Slices were cut 24 h after training.

CTA. CTA training took place in the light part of the cycle 7 d after surgery. Mice were deprived of water for 24 h and then pretrained for 5 d to get their daily water ration within 40 min per d from two tubes (10 ml). HSV virus was infused into lateral amygdala on both sides 3 h after the second day of pretraining. Conditioning started 3 d after virus injection.

On the conditioning day, the two tubes were filled with 0.2% saccharin sodium salt (wt/vol, the taste conditioned stimulus) instead of water. The conditioned stimulus was presented for 20 min and mice were treated 20 min later with the malaise-inducing agent LiCl (0.06 M, 2% of body weight, intraperitoneal).

Testing for aversion to saccharin occurred 24 h later. Allatostatin/vehicle was infused 30 min before testing. Two tubes (one containing water and the other containing saccharin) were presented for 40 min. The intake of each fluid was measured and the aversion index, defined as (milliliters of water consumed)/(milliliters of water + milliliters of saccharin consumed) × 100%. The 50% aversion index is the equal preference level, and the higher the aversion index, the more the mice preferred water to saccharin.

Histology. After the behavioral experiments, mice were killed by transcardial perfusion with 4% paraformaldehyde in 0.1 M phosphate buffer (pH 7.4, wt/vol). Brains were sliced coronally (40 µm). The cannula tip locations were confirmed by crystal violet staining at the end of each experiment. Only those mice with bilateral placements in the basolateral complex of the amygdala were included in analysis.

Quantitative analyses of infection levels were performed using the US National Institutes of Health image processing system. Before confocal imaging, we used transmission light microscopy and the thalamo-lateral amygdala fibers and the cortico-lateral amygdala fibers to locate the dorsal and lateral boundary of the lateral amygdala. The total number of GFP-positive cells in the lateral amygdala was counted bilaterally with a fixed sample window (0.1 mm^2) across at least six sections from comparable anteroposterior levels from each mouse. To assess the number of nuclei in the areas counted, we re-stained the slices using 4′,6′-diamidino-2-phenylindole (DAPI) after washout of FITC-conjugated primary antibody to GFP. The percentage of GFP-positive cells was calculated as the percentage of GFP-positive cell per total DAPI-labeled nuclei in the lateral amygdala. After the immunofluorescent studies, brain slices were counter stained with crystal violet to confirm the position of the infusion cannula.

Electrophysiology. Brains were rapidly removed from adult mice (3–4 months old) 2–3 d after virus infusion and placed in ice-cold ACSF containing 120 mM NaCl, 20 mM $NaHCO_3$, 3.5 mM KCl, 1.25 mM NaH_2PO_4, 2.5 mM $CaCl_2$, 1.3 mM $MgSO_4$ and 10 mM D-glucose. Coronal slices (400 µm thick) containing the amygdala were prepared and allowed to recover in oxygenated (95% O_2/5% CO_2) ACSF at 25–29 °C for at least 1 h before experiments were performed. All solutions were bubbled with 95% O_2/5% CO_2 and perfused over the slice at a rate of ~2 ml min^{-1} at 31 °C. Cells were visualized with an upright microscope using infrared or epifluorescent illumination, and whole-cell current-clamp recordings were made from neurons in the lateral amygdala with a Dagan 3900A amplifier and Multiclamp 700A. Electrodes (3–6 MΩ) contained 120 mM potassium methansulfate, 20 mM KCl, 10 mM HEPES, 0.2 mM EGTA, 2.0 mM $MgCl_2$, 2 mM Mg_2ATP, 0.3 mM Na_3GTP, 7 mM phosphocreatine (pH 7.2–7.4, 290–300 mOsm). Alexa 568 (0.2 mg ml^{-1}, Molecular Probes) was included in the internal solution. Responses were filtered at 2 kHz and digitized at 10 kHz. All data were acquired, stored and analyzed using pClamp9.0 (Axon Instruments) and Matlab (R2007a). Access resistance was monitored throughout the experiment. Input resistance was monitored throughout the experiment by applying a hyperpolarizing current (–100 pA). Only cells that reached the minimal criteria for health and stability (resting membrane potential more negative than −55 mV and access resistance less than 20 MΩ) were included in the analyses of this study.

Pyramidal neurons in lateral amygdala were identified on the basis of their action potential half-width and spike frequency adaptation in response to a long depolarizing current injection, as described previously[24]. Cell passive membrane properties were examined at resting potential. The spike amplitude, half-width and spike threshold were measured from the first spike in each trace that showed the smallest number of evoked spikes (usually only one spike) in response to a depolarizing step (either 50, 100 or 150 pA, 600 ms). Spike amplitudes were measured from resting potential. The threshold for spike initiation was taken as the beginning of the upstroke of the action potential. Action potential half-widths were measured as the spike width at the half-maximal voltage. Input resistance was calibrated by fitting the *I-V* curve with a linear regression. To investigate the

doi:10.1038/nn.2405

firing properties of neurons, we delivered 15 current injection steps (600-ms duration) from −200–500 pA in 50-pA increments. This protocol was repeated three times to obtain stable responses. In the allatostatin experiments, this protocol was repeated six times, twice to obtain control responses, twice after the application of allatostatin and repeated twice again after washout of allatostatin. The lateral amygdala cells that we recorded were further divided into two groups on the basis of spike-frequency adaptation[24]. Rapidly adapting cells fired only 1–5 spikes at the onset of the current injection (600 ms, 400 pA) and remained silent for the rest of the current pulses. Slowly adapting cells fired more than six spikes. Post-burst AHPs were evoked in current clamp by applying a 50-ms suprathreshold stimulation (≥400 pA, mostly 400 pA) current step from a holding potential of −60 mV to induce at least two spikes[42,43]. Cells that fired only once with varying injection currents were excluded from further analysis. The AHPs were measured at two time points: the negative peak of the AHP and 300 ms after the end of the 50-ms pulse. Drugs were applied by adding them to the superfusate at the appropriate concentration. Because the neuronal excitability of uninfected cells in HSV-CREB mice (n = 40 neurons, 8 mice), HSV-LacZ vector–transfected cells (n = 12 neurons, 2 mice) and nearby uninfected cells (n = 12 neurons, 2 mice) were not significantly different ($P > 0.05$), we pooled the data and used it as a control.

The thalamo-lateral amygdala pathway was stimulated with a bipolar platinum electrode. The distance between the recording and stimulating sites was between 150 and 450 μm. We delivered 100-μs stimuli at 10-s intervals. For the basal synaptic transmission studies, the input-output curve was constructed by varying stimulus intensity (10–100 μA) and measuring the corresponding EPSC amplitude. Peak EPSC was measured as the peak inward current. For PPF studies, the peak amplitude for individual responses was measured as the difference between the current level before the stimulus artifact and the peak of the EPSC[18]. Stimulation position and intensity were set to evoke an EPSC of ~50–200 pA. For experiments carried on trained mice, the same training protocol (see tone fear conditioning section) was applied and recordings were conducted 24 h after training.

To compare the AMPA/NMDA ratio of evoked synaptic transmission, we measured the AMPA component as the EPSC peak amplitude at −70 mV; the NMDA component was determined by measuring the current amplitude at 100 ms after EPSC onset at 30 mV[44]. Stimulation position and intensity were set to evoke an EPSC of ~50–200 pA. In the AMPA/NMDA ratio study, experiments were performed in the presence of the $GABA_A$ receptor blocker picrotoxin (100 μM).

For synaptically evoked excitability studies, series of pulses (at least 60 pulses, 10 pulses for each stimulation intensity) were given at each of the stimulation intensities used (covering a range of responses from subthreshold to supramaximal). E-S curves were constructed by binning the totality of the EPSP slopes and plotting the average of the bin versus the percentage of successful action potentials in that bin[29]. Stimulation intensities ranged from 30 to 300 μA. The data points were fit with a sigmoid, $S = 1/(1+ \exp[(E_{50} - E)/K])$, where E_{50} is the EPSP slope that yields action potentials 50% probability (the input-output threshold). The gain was determined by calculating the slope of the linear potion of the sigmoid.

Statistical analysis. Results are expressed as mean ± s.e.m. ANOVA analyses or t tests were used for statistical comparisons between groups as described in the context. $P < 0.05$ indicates significant difference between groups.

39. Lim, F. & Neve, R.L. *Current Protocols in Neuroscience* (Greene Publishing Assoc. and Wiley-Interscience, New York, 1999).
40. Paxinos, G. & Franklin, K.B.J. *The Mouse Brain in Stereotaxic Coordinates* (Academic Press, San Diego, 2003).
41. Barrot, M. *et al.* CREB activity in the nucleus accumbens shell controls gating of behavioral responses to emotional stimuli. *Proc. Natl. Acad. Sci. USA* **99**, 11435–11440 (2002).
42. Faber, E.S. & Sah, P. Opioids inhibit lateral amygdala pyramidal neurons by enhancing a dendritic potassium current. *J. Neurosci.* **24**, 3031–3039 (2004).
43. Liebmann, L. *et al.* Differential effects of corticosterone on the slow afterhyperpolarization in the basolateral amygdala and CA1 region: possible role of calcium channel subunits. *J. Neurophysiol.* **99**, 958–968 (2008).
44. Humeau, Y. *et al.* A pathway-specific function for different AMPA receptor subunits in amygdala long-term potentiation and fear conditioning. *J. Neurosci.* **27**, 10947–10956 (2007).